

# Molecular dynamics of water transport through membranes: Water from solvent to solute

Herman J.C. Berendsen and Siewert-Jan Marrink

BIOSON Research Institute and Department of Biophysical Chemistry, the University of Groningen, Nijenborgh 4, 9747 AG GRONINGEN, the Netherlands.

## Abstract

An application of Molecular Dynamics computer simulation (MD) to the process of transport of water through a lipid bilayer membrane is described. The permeation process is far too slow to be modeled by straightforward MD. In stead the inverse of the permeability coefficient is expressed as an integral over a local permeation resistance, which itself is inversely proportional both to the local density and the local diffusion constant. These quantities are recovered from MD simulations. The local density relates to a free energy profile, which is constructed by a combination of density determination, of the mean force on constrained molecules, and particle insertion. Thus a slow process can be accurately predicted from relatively short MD simulations.

## 1. INTRODUCTION

This presentation concerns a computer simulation study, using molecular dynamics (MD), of the transport of water through a bilayer membrane, in this case consisting of dipalmitoyl phosphatidylcholine (DPPC, lecithin). On the one hand this process is of considerable biological interest and on the other hand it poses a methodological challenge. The challenge is twofold. The first challenge is to perform a reliable MD simulation of a lipid bilayer in its liquid crystalline state using atomic detail of lipid molecules and solvent. Section 2 reviews such simulations as they have been performed in our laboratory over the past decade. The second challenge is to model a process (water penetration) that is very slow on the time scale of the simulation: during a simulation of typically one hundred picoseconds, it may happen once or twice, or not at all, that a water molecule will wander through the bilayer. Thus no statistics at all can be obtained on the permeation process. In section 3 the permeation process is described in the diffusion limit in terms of the thermodynamics of irreversible processes; this yields the key to computation of the permeability coefficient by combining the depth profiles over the membrane of free energy and diffusion. Sections 4 and 5 explain how these profiles can be determined from MD simulations. In Section 6 the results of both free energy and diffusion simulation are combined to obtain the permeation coefficient. A full account of this research is given in ref. [1].

## 2. MD SIMULATION OF LIPID BILAYERS

Simulation of lamellar liquid-crystalline systems has been a subject of research in our laboratory for over a decade, starting with a simplified bilayer of decane chains without detailed modeling of head groups and solvent [2,3], via detailed dynamics of multilamellar mesophases of sodium decanoate/decanol/water systems [4-6] to atomic simulations of DPPC in water [6,7]. The nature of the 'hydration force' between DPPC bilayers has also been investigated [8] and found to be related to the ordering of water by the interfacial dipolar charges.

The stability of the bilayers and their aggregation phase depend critically on details of the force field used. Lecithin bilayers can exist in (at least) two phases: a low-temperature *gel* phase in which the hydrocarbon chains are ordered but the head groups are still fluid, and a *liquid-crystalline* or phase in which the hydrocarbon chains are also fluid. With the standard GROMOS force field [9], DPPC was found to equilibrate towards the gel state, even at a temperature of 350 K, well above the phase transition temperature between gel and liquid-crystalline state. It was found necessary to make two modifications in order to obtain the liquid-crystalline phase at 350K: use a more accurate description of the dihedral angle function in the hydrocarbon chains, and reduce the ionic charges (on phosphate and choline) by a factor of two. The latter has the same effect as using a dielectric constant of 4 for the interactions of charges; this compensates partly for the lack of explicit polarisability in the force field. The DPPC simulations and its force field aspects have been recently reviewed [10].

The simulations were carried out in a rectangular periodic box using an algorithm that effects a coupling to a 'bath' of constant pressure and constant temperature [11]. The dimensions of the box adjust themselves to be consistent with the set pressure (1 atmosphere). While the overall density quickly equilibrates, the depth of the box, related to the thickness of the bilayer, takes several hundred picoseconds to equilibrate. It is in fact the slowest and most sensitive indicator of equilibrium, requiring the equilibration of rotational chain isomerism which takes place on the time scale of tens of picoseconds. It was found that either a gel or a liquid-crystalline phase could be obtained, depending on force field and temperature. The two-dimensional radial distribution function of chains showed a much stronger evidence of hexagonal packing in the gel than in the liquid-crystalline phase. The equilibrium surface areas for the two phases are in good agreement with experimental data: 0.485 nm<sup>2</sup> for the gel phase (experimental value 0.48) and 0.575 nm<sup>2</sup> for the liquid-crystalline phase (experimental value 0.60).

Another sensitive comparison with experiment can be made by computing the *deuterium resonance order parameters* which can be obtained from deuterium magnetic resonance line splittings. The order parameter  $S_{CD}$  that is measured is an average over the second spherical harmonic function of the angle  $\theta$  between the direction of the CD-bond and the membrane normal:

$$S_{CD} = \frac{1}{2}(3 \cos^2 \theta - 1)$$

Such order parameters can be obtained for all carbon atoms of the chain except the terminal ones. For a fully ordered, extended, non-tilted chain, the order parameter attains the value of -0.5; for an isotropically disordered chain its value is zero. Order parameters typically show a plateau value for the first half of the chain, tapering off to lower values towards the tail end of the chain. Well-ordered model systems like sodium decanoate/decanol/water have plateau values of about -0.3; in the less well-ordered lecithin bilayers the order parameters are around -0.2 in the liquid-crystalline phase. We have found almost exact agreement with experiment both for the model system simulations [5] and the lecithin simulations [6,7]. This gives confidence in those results that cannot be tested by experiment.

Fig. 1 shows a projection of a typical snapshot of the lecithin bilayer. There is more disorder than biochemistry text books suggest. The head group region spreads over about 0.7 nm and the interface has a fluctuating corrugated structure. A film conveys the fluctuations in the structure much better than a picture of this kind can do<sup>1</sup>. Four different zones, indicated in Fig. 1, can be distinguished:

**Region 1** Here the head groups start to appear, but still at low density. The water density decreases to about half the bulk value.

**Region 2** This is the region where the head group density is high and the water density decreases to almost zero. Hydrocarbon chains begin to appear.

**Region 3** This is the well-ordered and rather dense region of the hydrocarbon chains. The density here drops from 1.1 to about 0.75 g/cm<sup>3</sup>, typical for liquid decane.

**Region 4** In this tail region with its high proportion of methyl end groups, the density drops to about 0.6, typical for liquid ethane.

<sup>1</sup> A copy of a 7 minute video film can be obtained for US \$ 40,- from BIOMOS bv, Nijenborgh 4, 9747 AG GRONINGEN, the Netherlands

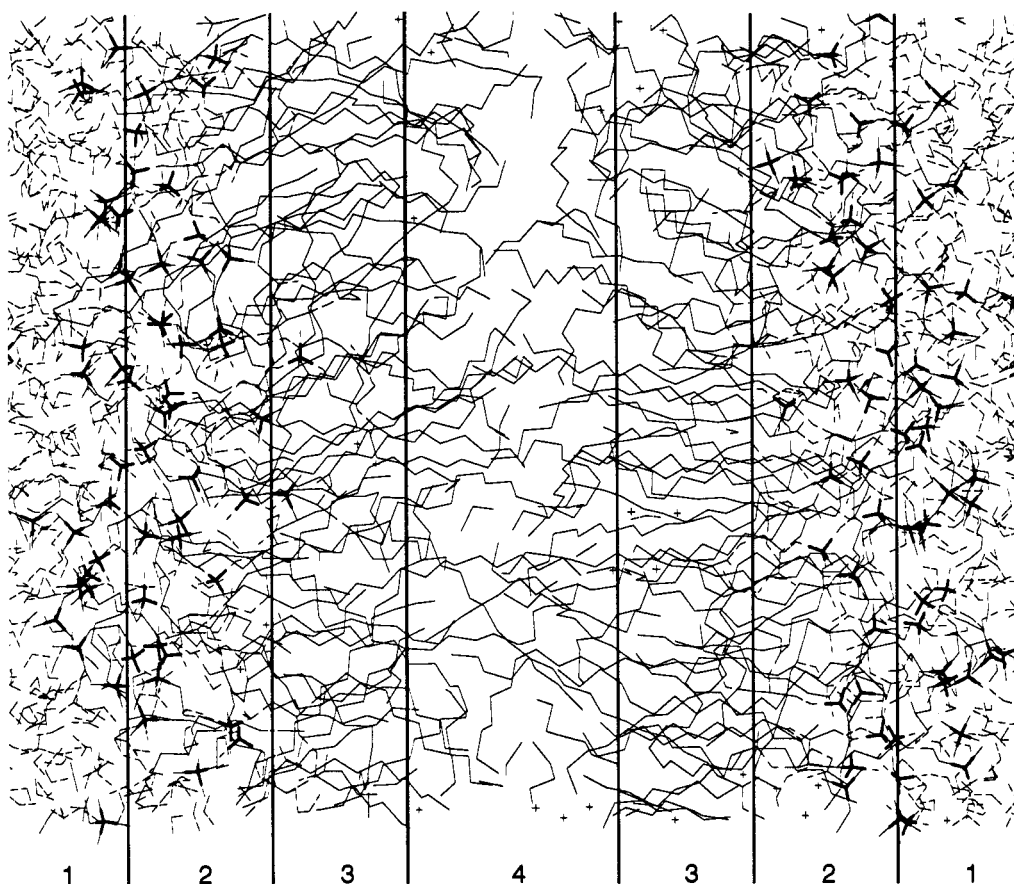


Figure 1: Snapshot of a lecithin bilayer. Choline and phosphate groups are highlighted. Water molecules are dashed V-shaped particles

The density profile in terms of electrons per unit volume agrees with the experimental profile determined from x-ray diffraction measurements on multilamellar phases. The density in the tail region is quite low and allows for a few percent free space for a probe molecule of the size of a water molecule [1].

### 3. TRANSPORT THROUGH MEMBRANES: A THERMODYNAMIC DESCRIPTION

During a simulation of typically 100 ps, it occurs once or twice that an isolated water molecule 'dissolves' into the membrane hydrocarbon phase, where it can diffuse quite easily. We never observed a cluster of two or more water molecules in the interior of the membrane, detached from the bulk aqueous medium. Thus it seems that the major transport of water takes place by permeation of single water molecules, although a very infrequent occurrence of permeating clusters or even of a complete pore by thermal fluctuation cannot be excluded on the basis of these simulations alone. It is clear that water permeation cannot be studied quantitatively by observing this process in an equilibrium simulation. Therefore we resort to a different approach. The permeation process is considered as a diffusion process in an external field, described as a free energy profile or *potential of mean force*. Our first concern is to describe the diffusional theory of transport in terms of the thermodynamics of irreversible processes. This enables us to link the permeation coefficient to experiments as well as to an integral over local properties in the inhomogeneous membrane.

### 3.1 General diffusional theory of transport

We consider the motion of particles of the  $i$ -th species (in this case water, but the theory is applicable to any solute as well) in the diffusional limit, where the *average velocity*  $\mathbf{u}_i = \langle \mathbf{v}_i \rangle$  is proportional to the thermodynamic *driving force*, which is the negative gradient of the thermodynamic potential  $\mu_i$ :

$$\mathbf{u}_i = -\frac{1}{\zeta_i} \nabla \mu_i \quad (1)$$

where  $\zeta_i$  is the frictional coefficient of the particles. [Note that, if the thermodynamic potential is expressed in J/mol, the frictional coefficient is expressed per mole of particles as well]. The flux  $J_i$  in mole  $\text{m}^{-2} \text{s}^{-1}$  is given by

$$J_i = c_i \mathbf{u}_i = -\frac{c_i}{\zeta_i} \nabla \mu_i \quad (2)$$

The friction coefficient  $\zeta_i$  is related to the diffusion constant  $D_i$  by

$$\zeta_i = RT/D_i \quad (3)$$

as can be easily seen when a concentration gradient in an ideal solution is considered for which  $\mu = \mu_0 + RT \ln c$  and eq. 2 is compared to Fick's law  $\mathbf{J} = -D \nabla c$ . The linear flux relations for the case that material properties depend on one coordinate  $z$  can now be written as

$$J_i(z) = -\frac{c_i(z) D_i(z)}{RT} \frac{d\mu_i(z)}{dz} \quad (4)$$

Together with a continuity equation, eq. 4 predicts the spatial and temporal evolution of the local density distribution. We are, however, interested in the *steady state* solution of the flux in the linear regime, *i.e.*, under the influence of a small deviation from equilibrium. Steady state means that  $J_i$  is not a function of  $z$ , and after rearranging we can integrate eq. 4 over the membrane from  $z_1$  in the bulk phase on one side to  $z_2$  in the bulk phase on the other side:

$$\Delta \mu_i = \mu_i(z_2) - \mu_i(z_1) = -J_i RT \int_{z_1}^{z_2} \frac{dz}{c_i(z) D_i(z)} \quad (5)$$

Here  $c_i(z)$  is the concentration of component  $i$  in the presence of the imposed gradient. Under the assumption of small gradients we can replace this concentration by the *equilibrium concentration*  $c_i^{eq}$  in the absence of an imposed gradient.

If we define the *permeation resistance*  $R_i^p$  as

$$R_i^p = c_i^* \int_{z_1}^{z_2} \frac{dz}{c_i^{eq}(z) D_i(z)} \quad (6)$$

where  $c_i^*$  is the concentration in the bulk solutions on either side of the membrane in the absence of an imposed gradient, the linear response relation, eq. 5, becomes

$$J_i = -\frac{c_i^*}{R_i^p} \frac{\Delta \mu_i}{RT} \quad (7)$$

The permeation resistance is directly related to the experimental *permeability coefficient* (section 3.2), and is also amenable to computation on the basis of detailed simulation. For the latter the calculation of the local equilibrium density  $c_i^{eq}(z)$  (section 4) and the local diffusion constant (section 5) are separate tasks that must be accomplished first before eq. 6 can be integrated. The result of the integration is given in section 6.

Before proceeding, let us summarise the *assumptions* that have been made either explicitly or implicitly in the derivations thus far:

- (1) The whole system is isothermal at absolute temperature  $T$
- (2) The membrane component is stationary in the frame of reference
- (3) The local diffusional model is valid: the thermodynamic gradient can be considered constant over the *correlation distance* of the particle (the distance given by the displacement of a particle during the time over which its velocity correlation function differs from zero)
- (4) The fluxes are proportional to the gradients in thermodynamic potential. This means that the limit of small gradients is considered where this is needed.
- (5) The permeation process for water is dominated by single molecules that only feel friction with the stationary membrane component.

Assumption (3) is the most questionable one, because the concentration gradients in a membrane are very large and the diffusion is relatively fast. It is possible to refine the barrier-crossing dynamics by including details of the velocity (or force) autocorrelation of the particles [12], but we restrict our considerations to the simple diffusional limit.

### 3.2 Experimental quantities

The driving force for permeation processes can be imposed by the following causes: hydrostatic pressure difference  $\Delta p$  (water), osmotic pressure difference  $\Delta\Pi$  (water), or concentration difference  $\Delta c$  (solute or water isotope). Hydrostatic and osmotic differences are equivalent in their influence on the thermodynamic potential of water:

$$\Delta\mu_w = (\Delta p - \Delta\Pi)/c_w^* \quad (8)$$

Comparing eq. 7 with eq. 8, the flux can be expressed as

$$J_w = -\frac{1}{R_w^p} \frac{(\Delta p - \Delta\Pi)}{RT} \quad (9)$$

For the flux  $J_i$  of an isotope  $i$  of water, we consider the  $z$ -dependent mole fraction  $x_i(z)$  of the isotope. Its thermodynamic potential is given by

$$\mu_i(z) = \mu_w(z) + RT \ln x_i(z) \quad (10)$$

Assuming water to be in equilibrium over the membrane,  $\mu_w$  is constant and equal to its bulk value  $\mu_w^*$ . Integration of eq. 4 using eq. 10 and equating  $c_i(z)$  with  $x_i(z)c_w(z)$ , we find

$$J_i = -\frac{1}{R_w^p} \Delta c_i, \quad (11)$$

where  $\Delta c_i = c_w^* \Delta x_i$  is the concentration difference of the isotope across the membrane.

For the flux of a solute resulting from a (small) concentration difference  $\Delta c_s$  over the membrane, for which

$$\Delta\mu_s = RT \frac{\Delta c_s}{c_s^*} \quad (12)$$

it is easily derived that

$$J_s = -\frac{1}{R_s^p} \Delta c_s \quad (13)$$

The permeability coefficient  $P$  is usually defined as the ratio between flux and concentration difference, and thus  $P$  is equivalent to the inverse of the permeation resistance  $R_i^p$  defined by eq. 6:

$$R_i^p = 1/P \quad (14)$$

Experimental values of  $P$  for lecithin membranes range from  $2.5 \times 10^{-3}$  to  $2.5 \times 10^{-2}$  cm/s, with a value of  $8 \times 10^{-2}$  cm/s for the red blood cell membrane, if corrected to 350 K, the temperature of the simulation [1].

## 4. COMPUTATION OF EQUILIBRIUM LOCAL DENSITY

We now consider how the local equilibrium water concentration, expressed as a ratio to the bulk concentration,  $c_w^{\text{eq}}(z)/c_w^*$ , as it figures in the integrand of eq. 6, can be computed from simulations<sup>2</sup>. The quantity  $c dz$  is proportional to the probability that the system resides in phase space with the restriction that the  $z$ -coordinate of one particular water molecule (call it nr 0:  $z_0$ ), occurs in the interval  $(z, z + dz)$ . The local concentration is therefore proportional to the *constrained partition function*  $Q'$ :

$$Q'(z) = a \int d\mathbf{r}_1 \dots d\mathbf{r}_N \delta(z_0 - z) \exp \{-V(\mathbf{r}_1 \dots \mathbf{r}_N)/kT\} \quad (15)$$

where  $a$  is a constant. The ratio  $c(z)/c^*$  is given by the ratio of  $Q'(z)$  and  $Q'(z_1)$  at position  $z_1$  in the bulk

<sup>2</sup>from here on we drop the superscript and subscript; concentrations refer to water in the equilibrium state.

solution. This ratio can be related to the *potential of mean force*  $\Delta G$  relative to the bulk phase:

$$\Delta G(z) = -RT \ln \frac{Q'(z)}{Q'(z_1)} = -RT \ln \frac{c(z)}{c^*}. \quad (16)$$

Thus the permeation resistance, eq. 6, can also be expressed in the potential of mean force

$$R_i^p = \int_{z_1}^{z_2} \frac{\exp(\Delta G(z)/RT)}{D_i(z)} dz \quad (17)$$

In practice the potential of mean force (or, equivalently, the local concentration) cannot be computed from simulations by a single method, because any method has its limited range of accuracy. There are several different methods, of which we have used three (described below) in three distinct regions of the membrane. A fourth possible method is *umbrella sampling*, which restricts the sampling of phase space to a narrow region in the membrane depth, and a fifth method is *thermodynamic integration* which measures the free energy needed to materialise a particle at a given point in space. The results are given in section 6.

#### **Analysis of local density**

In regions 1 and 2 of the membrane the water concentration can be determined directly with sufficient accuracy, and  $\Delta G(z)$  follows immediately from eq. 16. The membrane is sectioned into slices and the number of water molecules is counted per slice and averaged over the length of the simulation. The statistics of particle counting can be assumed to follow a Poisson distribution.

#### **Particle insertion**

In regions where the density is low and some free space is available (as in the middle of the membrane), the standard free energy can be found by *particle insertion* [13]. The procedure is to insert a water molecule as a 'ghost' particle, *i.e.*, without disturbing the configuration, randomly into the region of interest and determine its interaction energy  $E^{ins}$  with the 'real' particles. Now define its Boltzmann factor, averaged over many insertions, as the *insertion thermodynamic potential*:

$$\Delta \mu^{ins} = -RT \ln(\exp(-E^{ins}/kT)), \quad (18)$$

In the case of a very dilute solution  $\Delta \mu^{ins}$  measures the difference in standard thermodynamic potential of the solution (of water in the membrane phase) and the ideal gas, referred to the same standard concentration:

$$\mu^0(\text{solution}) = \mu^0(\text{ideal gas}) + \Delta \mu^{ins} \quad (19)$$

In the parts of the membrane where particle insertion is possible, water is so dilute that it forms an ideal solution with concentration  $c(z)$ , which is in equilibrium with bulk water outside the membrane, with thermodynamic potential  $\mu^*$ :

$$\mu^* = \mu^0(\text{solution}) + RT \ln c(z) \quad (20)$$

From eqs 16, 19, and 20 it follows that

$$\Delta G(z) = \Delta \mu^{ins}(z) + [\mu^0(\text{ideal gas}) + RT \ln c^* - \mu^*] \quad (21)$$

Eq. 21 shows that the potential of mean force can be 'measured' by the insertion thermodynamic potential, but shifted by a correction term, given between the brackets  $[\dots]$  in eq. 21. The correction term is constant at a given temperature and was found to be +24.3 kJ/mol for the water model used (SPC model [14]) by thermodynamic integration [15]. Its experimental value, assuming ideality of the saturated vapour, is equal to

$$[\dots] = RT \ln \left\{ \frac{RTc^*}{p_{sat}} \right\}, \quad (22)$$

where  $p_{sat}$  is the saturated vapour pressure or, more accurately, its fugacity. For  $T = 300\text{K}$  (density  $996.57 \text{ kg/m}^3$ ;  $p_{sat} = 3567 \text{ Pa}$ ) the correction term is 26.35 kJ/mol and for  $T = 350\text{K}$  (density  $973.61 \text{ kg/m}^3$ ,  $p_{sat} = 41905 \text{ Pa}$ ) it is 23.95 kJ/mol.

#### **Average force on constrained particle**

Where neither density determination nor particle insertion give accurate results, it is possible to find the *derivative* of the potential of mean force by measuring the average force exerted on a water molecule that is *constrained* at a given depth  $z$  in the membrane. This follows by taking the derivative of  $\Delta G$  (eq. 16):

$$\frac{d\Delta G}{dz} = -\frac{RT}{Q'(z)} \frac{dQ'(z)}{dz} \quad (23)$$

The derivative of  $Q'$  is found by partial integration of eq. 15 to be

$$\frac{dQ'(z)}{dz} = -\frac{a}{kT} \int dr_1 \dots dr_N \delta(z_0 - z) \frac{\partial V}{\partial z_0} \exp\left(-\frac{V}{kT}\right) \quad (24)$$

Hence

$$\frac{d\Delta G}{dz} = N_{Av} \langle F_z \rangle, \quad (25)$$

where  $\langle F_z \rangle$  is the mean force on the constraint (*i.e.*, the component of the force on the water molecule in the direction of the constraint  $z$ , averaged over the constrained ensemble). This force is easily monitored during a constrained simulation: The constraint is imposed by resetting the  $z$ -coordinate of the center-of-mass of a water molecule each step to its original, constrained, value (with respect to the center-of-mass of the system); the force is directly proportional to the distance over which the  $z$ -coordinate is reset. The force fluctuates heavily, but a long simulation nevertheless provides accurate averages.

## 5. LOCAL DIFFUSION CONSTANTS

Normally, the diffusion constant of a particle is best determined from an MD simulation by observing its mean square displacement as a function of time and determining  $D$  from the limiting slope. The determination of a *local* diffusion constant is not obvious, because during the observation of its displacement the particle wanders through regions with different diffusion constants. If only those particles are selected that remain in a given region during a sufficiently long time, an unacceptable bias is introduced. An alternative method relates the diffusion constant to the integral of the force autocorrelation function, which can be obtained from the simulations with constrained water molecules [1]. It was found to be possible to determine local diffusion constants in the membrane by both methods, which agree within statistical error. It was found that the diffusion constants in the  $z$ -direction are very similar to those in the  $x, y$ -directions [1].

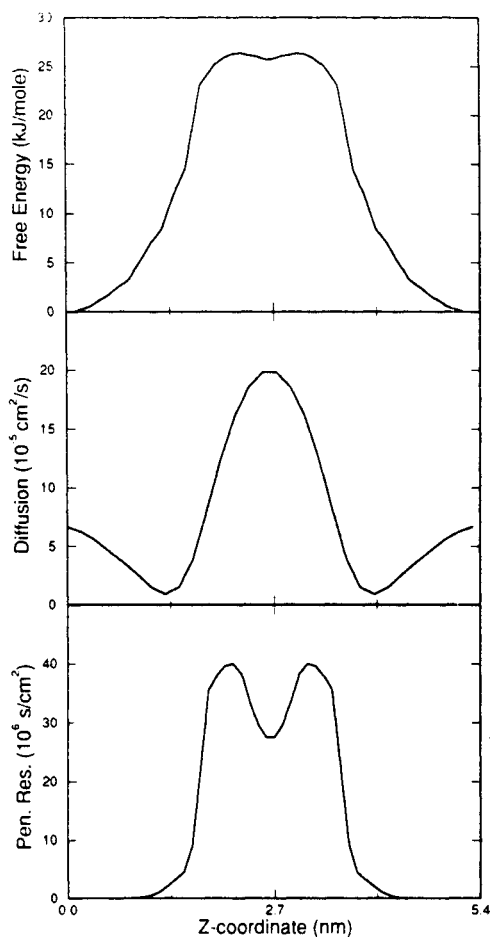


Figure 2: The free energy profile (top), the diffusion profile (middle), and the permeation resistance profile (bottom) for water penetration through a lecithin bilayer. From ref 10.

## 6. RESULTS ON WATER PERMEATION THROUGH A LIPID BILAYER

Figure 2 shows the results of the free energy profile, the profile of local diffusion constant, and the profile of the resulting local permeation resistance. The free energy barrier amounts to some 25 kJ/mol, which means that the density of water in the middle of the membrane is comparable to the density of water in the saturated vapour. The diffusion constant varies considerably with the depth in the membrane: near the headgroups (region 3) the diffusion is rather restricted, but in the middle of the bilayer diffusion is faster than in bulk water. The latter is related to the occurrence of a few percent free space in the middle of the bilayer. The total permeation resistance obtained by integrating the local resistance (eq.6) has the value of 0.08 cm/s, which is slightly above the range of experimental values. The bottleneck for permeation appears to be concentrated in the rather dense region 3 of the chains just behind the head groups, while the middle of the bilayers present less of a resistance to permeation. The effective thickness of the membrane for water penetration is roughly 2 nm.

We have shown that it is quite feasible to study a slow mechanism as membrane permeation by relatively short molecular dynamics simulations, by evaluating transport coefficients and local thermodynamic potentials. These two types of quantities lie at the basis of *mesoscopic* dynamic theories that are able to study aggregation behaviour and micro-phase separation kinetics in complex systems on a much larger time- and length scale than molecular dynamics can ever provide. In our laboratory Fraaije is pioneering such theories using a (classical) density functional approach to describe the local thermodynamic potentials. His results [16] show that the slow phase separation of random copolymer melts can be perfectly simulated by this mesoscopic dynamics, opening a new and promising field of research.

### Acknowledgements

This work was supported in part by the Foundation for Biophysics, under the auspices of the Netherlands Research Organisation, NWO.

### REFERENCES

1. S.J. Marrink and H.J.C. Berendsen, *Simulation of water transport through a lipid membrane*, submitted 1993.
2. P. van der Ploeg and H.J.C. Berendsen, *J. Chem. Phys.* **76**, 3271-3276 (1982).
3. P. van der Ploeg and H.J.C. Berendsen, *Mol. Phys.* **49**, 233-248 (1983).
4. H.J.C. Berendsen and E. Egberts, in *Structure, Dynamics and Function of Biomolecules*, A. Ehrenberg, R. Rigler, A. Gräslund and L. Nilsson, eds, (Springer Verlag, Berlin, 1986), pp 275-280.
5. E. Egberts and H.J.C. Berendsen, *J. Chem. Phys.* **89**, 3718-3732 (1988).
6. E. Egberts, *Molecular Dynamics Simulation of Multibilayer Membranes*, Ph.D. Thesis, University of Groningen, 1988
7. E. Egberts, S.J. Marrink and H.J.C. Berendsen, *Eur. Biophys. J.*, in print 1993.
8. S.J. Marrink, M. Berkowitz and H.J.C. Berendsen, *Langmuir*, in print 1993.
9. W.F. van Gunsteren and H.J.C. Berendsen, *GROMOS87 manual*, BIOMOS b.v., Nijenborgh 4, 9747 AG GRONINGEN, the Netherlands.
10. H.J.C. Berendsen, E. Egberts, S.J. Marrink and P. Ahlström, in *Membrane Proteins: Structure, Interactions and Models*, B. Pullman *et al.* eds., Kluwer Acad. Publ. 1992, pp 457-470.
11. H.J.C. Berendsen, J.P.M. Postma, W.F. van Gunsteren, A. DiNola and J. R. Haak, *J. Chem. Phys.* **81**, 3684-3690 (1984).
12. K. Schulten, Z. Schulten and A. Szabo, *J. Chem. Phys.* **74**, 4426-4432 (1981)
13. B. Widom, *J. Chem. Phys.* **39**, 2802 (1963)
14. H.J.C. Berendsen, J.P.M. Postma, W.F. van Gunsteren and J. Hermans, In *Intermolecular Forces*, B. Pullman, ed., Reidel Publ., Dordrecht 1981, pp 331-342
15. J. Hermans, A. Pathiaseril and A. Anderson, *J. Am. Chem. Soc.* **110**, 5982 (1988)
16. J.G.E.M. Fraaije, *J. Chem. Phys.*, in press 1993